CHEMICAL ENGINEERING TRANSACTIONS Volume 17, 2009
Editor Sauro Pierucci
 ISBN 978-88-95608-01-3 ISSN 1974-9791
DOI: 10.3303/CET0917018

Modelling of dynamic processes during the regeneration of NO_X storage catalyst

Petr Kočí[1,*], Jan Štěpánek[1], František Plát[1], Miloš Marek[1], Milan Kubíček[2]
[1]Department of Chemical Engineering, [2]Department of Mathematics,
Center for Nonlinear Dynamics of Chemical and Biological Systems,
Institute of Chemical Technology, Prague,
Technická 5, CZ 166 28 Prague, Czech Republic
*Corresponding author, e-mail: petr.koci@vscht.cz, http://www.vscht.cz/monolith

Two kinetic models for the NO_X reduction in periodically operated NO_X storage catalyst are discussed – the simpler NH_3-selectivity model, and the more complex NH_3-dynamics model. They differ in the approach to the formation of the NH_3 as a main by-product of the stored NO_X reduction. The NH_3-selectivity model assumes direct reduction of the stored NO_X to nitrogen or ammonia with empirically obtained selectivity ratio, dependent on temperature and the reducing agent (CO, H_2 and HC). The more complex NH_3-dynamics model considers both NH_3 formation and NH_3 decomposition reactions in the spatially distributed system, resulting in the evolution of moving NH_3 peak on the reduction front boundary during the NSRC regeneration. The predictions of the two models are compared and confronted with experimental observations. For the estimation of integral component conversion (cumulative emissions) around the mean regeneration phase length the simpler NH_3-selectivity model can be used. The more complex NH_3-dynamics model is consistent with experimentally observed evolution of the outlet NH_3 concentrations, and it is also more sensitive to operating conditions. On the other hand, the increased model complexity results in longer computation times.

1 Introduction

Lean-burn (mainly Diesel) engines are more fuel efficient than the ones burning stoichiometric air-fuel mixture, but they produce also significant amount of nitrogen oxides that cannot be removed in a conventional three-way catalyst due to the excess of oxygen in the exhaust gas. For abatement of NO_X emissions from lean-burn engines, two main catalytic arrangements can be utilized: the urea-selective catalytic reduction (SCR), and the NO_X storage and reduction catalyst (NSRC). These catalysts can be used together and combined with other converter types (mainly oxidation catalyst and particulate filter) to improve the overall efficiency of the exhaust gas aftertreatment system (Güthenke et al., 2007a).

The NSRC needs periodic regeneration for correct operation. Normally, the engine runs in lean mode (with excess of oxygen), which improves the vehicle fuel economy, but hinders

Please cite this article as: Koci P., Stepanek J., Plat F., Marek M. and Kubicek M., (2009), Modelling of dynamic processes during the regeneration of nox storage catalyst, Chemical Engineering Transactions, 17, 105-110 DOI: 10.3303/CET0917018

direct reduction of nitrogen oxides. In this regime, the nitrogen oxides are being stored on the catalyst surface in the form of nitrites and nitrates (Epling et al., 2004). After few minutes the catalyst becomes saturated and needs to be regenerated. The engine control unit switches to rich regime (burning a mixture with excess of fuel) for a few seconds. During this rich phase the stored NO_x are desorbed and reduced by CO, H_2 and unburned hydrocarbons (HC) to N_2, or up to NH_3 (Kočí et al., 2008). It has been experimentally proved, that NH_3 plays an important role in the regeneration process because it can further react with the stored NO_x to produce N_2 (Cumaratunge et al., 2007). Ammonia is normally an undesired final product of the NO_x reduction because it is irritant. However, NH_3 can be adsorbed in an SCR converter placed downstream of the NSRC, and used for the additional NO_x reduction in the subsequent lean phase (Güthenke et al., 2007a).
In this contribution we compare two global NSRC kinetic models: (i) NH_3-selectivity model, assuming direct reduction of the stored NO_x to nitrogen or ammonia with empirically obtained selectivity ratio, dependent on temperature and the reducing agent (CO, H_2 and HC), and (ii) more complex NH_3-dynamics model, considering both NH_3 formation and NH_3 decomposition reactions in the spatially distributed system (Kočí et al., 2008).

2 Mathematical model of catalytic monolith

Heterogeneous, spatially 1-dimensional (1D) plug-flow model of catalytic monolith channel with surface component deposition (Güthenke et al., 2007a; Kočí et al., 2007) has been used for the simulations of catalytic monolith converter. The model considers the following balances: mass balances of individual components in the flowing gas (1), in the washcoat pores (2) and on the catalyst surface (3), total enthalpy balance of the flowing gas (4), the enthalpy balance of the solid phase (5), and boundary conditions (6)-(7):

$$\frac{\partial c_k(z,t)}{\partial t} = -\frac{\partial (v \cdot c_k)}{\partial z} + \frac{k_c a}{\varepsilon^g} c \left(y_k^s - y_k \right), \quad k = 1,\ldots,K \tag{1}$$

$$\frac{\partial c_k^s(z,t)}{\partial t} = \frac{k_c a}{\varepsilon^s (1-\varepsilon^g)\varphi^s} c \left(y_k - y_k^s \right) + \frac{1}{\varepsilon^s} \sum_{j=1}^{J} \nu_{k,j} R_j, \quad k = 1,\ldots,K \tag{2}$$

$$\frac{\partial \psi_m(z,t)}{\partial t} = \frac{1}{\Psi_m^{cap}} \sum_{j=1}^{J} \nu_{m,j}^{\psi} R_j, \quad m = 1,\ldots,M \tag{3}$$

$$\rho c_p \frac{\partial T(z,t)}{\partial t} = -v \frac{\partial T}{\partial z} \rho c_p + \frac{k_h a}{\varepsilon^g} \left(T^s - T \right) \tag{4}$$

$$\rho^s c_p^s \frac{\partial T^s(z,t)}{\partial t} = \lambda^s \frac{\partial^2 T^s}{\partial z^2} + \frac{k_h a}{1-\varepsilon^g} \left(T - T^s \right) - \varphi^s \sum_{j=1}^{J} \Delta H_{r,j} R_j \tag{5}$$

$$T = T^{in}, c_k = c_k^{in},\ k = 1 \ldots K \quad \text{at } z = 0 \tag{6}$$

$$\frac{\partial T^s}{\partial z} = 0 \quad \text{at } z = 0, L \tag{7}$$

Here a is density of external surface area in monolith, c molar concentration, c_p specific heat capacity, superscript "g" denotes gas phase, j is index of reaction, k index of gas component, k_c mass transfer coefficient, k_h heat transfer coefficient, L monolith length, m index of surface-deposited component, R_j reaction rate, superscript "s" denotes solid phase, t is time, T temperature, v linear gas velocity, y mole fraction, z spatial coordinate along monolith, ΔH_r reaction enthalpy, ε^g fraction of open frontal area in monolith, ε^s

Table 1: Reactions on NO_x storage and reduction catalyst – NH_3 selectivity model.

Reaction step	Reaction rate
$CO + \frac{1}{2}\ O_2 \rightarrow CO_2$	$R_1 = k_1\ y_{CO}\ y_{O_2}/G_1$
$H_2 + \frac{1}{2}\ O_2 \rightarrow H_2O$	$R_2 = k_2\ y_{H_2}\ y_{O_2}/G_1$
$C_3H_6 + \frac{9}{2}\ O_2 \rightarrow 3\ CO_2 + 3\ H_2O$	$R_3 = k_3\ y_{C_3H_6}\ y_{O_2}/G_1$
$CO + H_2O \rightleftharpoons CO_2 + H_2$	$R_4 = k_4\ [y_{CO} y_{H_2O} - y_{CO_2} y_{H_2}/K^{eq}_{y,4}]$
$C_3H_6 + 3\ H_2O \rightarrow 3\ CO + 6\ H_2$	$R_5 = k_5\ [y_{C_3H_6} y_{H_2O} - y^3_{CO} y^6_{H_2}/(K^{eq}_{y,5} y^2_{H_2O})]$
$CO + NO \rightarrow CO_2 + \frac{1}{2}\ N_2$	$R_6 = k_6\ y_{CO}\ \sqrt{y_{NO}}/G_1/G_2$
$H_2 + NO \rightarrow H_2O + \frac{1}{2}\ N_2$	$R_7 = k_7\ y_{H_2}\ \sqrt{y_{NO}}/G_1/G_2$
$C_3H_6 + 9\ NO \rightarrow 3\ CO_2 + 3\ H_2O + \frac{9}{2}\ N_2$	$R_8 = k_8\ y_{C_3H_6}\ \sqrt{y_{NO}}/G_1/G_2$
$NO + \frac{1}{2}\ O_2 \rightleftharpoons NO_2$	$R_9 = k_9\ [y_{NO}\ y^{0.5}_{O_2} - y_{NO_2}/K^{eq}_{y,9}]/G_1$
$Ce_2O_3 + \frac{1}{2}\ O_2 \rightarrow Ce_2O_4$	$R_{10} = k_{10}\ \Psi_{cap,O_2}\ y_{O_2}\ (\psi^{eq}_{O_2} - \psi_{O_2})$
$Ce_2O_4 + CO \rightarrow Ce_2O_3 + CO_2$	$R_{11} = k_{11}\ \Psi_{cap,O_2}\ y_{CO}\ \psi_{O_2}$
$Ce_2O_4 + H_2 \rightarrow Ce_2O_3 + H_2O$	$R_{12} = k_{12}\ \Psi_{cap,O_2}\ y_{H_2}\ \psi_{O_2}$
$Ce_2O_4 + \frac{1}{9}\ C_3H_6 \rightarrow Ce_2O_3 + \frac{1}{3}\ CO_2 + \frac{1}{3}\ H_2O$	$R_{13} = k_{13}\ \Psi_{cap,O_2}\ y_{C_3H_6}\ \psi_{O_2}$
$NO_2 + \frac{1}{2}\ O_2 + BaO \rightarrow Ba(NO_3)$	$R_{14} = k_{14}\ \Psi_{cap,NO_x}\ y_{NO_2}\ (\psi^{eq}_{NO_x} - \psi_{NO_x})^2$
$2\ NO + \frac{3}{2}\ O_2 + BaO \rightarrow Ba(NO_3)$	$R_{15} = k_{15}\ \Psi_{cap,NO_x}\ y_{NO}\ (\psi^{eq}_{NO_x} - \psi_{NO_x})^2$
$Ba(NO_3)_2 + 5\ CO \rightarrow N_2 + 5\ CO_2 + BaO$	$R_{16} = k_{16}\ \Psi_{cap,NO_x}\ y_{CO}\ \psi_{NO_x}/G_3/(1 + S^{CO}_{NH_3})$
$Ba(NO_3)_2 + 5\ H_2 \rightarrow N_2 + 5\ H_2O + BaO$	$R_{17} = k_{17}\ \Psi_{cap,NO_x}\ y_{H_2}\ \psi^2_{NO_x}/G_3/G_5/(1 + S^{H_2}_{NH_3})$
$Ba(NO_3)_2 + \frac{5}{9} C_3H_6 \rightarrow BaO + \frac{5}{3}\ CO_2 + \frac{5}{3}\ H_2O + N_2$	$R_{18} = k_{18}\ \Psi_{cap,NO_x}\ y_{C_3H_6}\ \psi^2_{NO_x}/G_3/(1 + S^{C_3H_6}_{NH_3})$
$Ba(NO_3)_2 + 3\ CO \rightarrow 2\ NO + 3\ CO_2 + BaO$	$R_{19} = k_{19}\ \Psi_{cap,NO_x}\ y_{CO}\ \psi_{NO_x}/G_4$
$Ba(NO_3)_2 + 3\ H_2 \rightarrow 2\ NO + 3\ H_2O + BaO$	$R_{20} = k_{20}\ \Psi_{cap,NO_x}\ y_{H_2}\ \psi_{NO_x}/G_4$
$Ba(NO_3)_2 + \frac{1}{3}\ C_3H_6 \rightarrow 2\ NO + CO_2 + H_2O + BaO$	$R_{21} = k_{21}\ \Psi_{cap,NO_x}\ y_{C_3H_6}\ \psi_{NO_x}/G_4$
$Ba(NO_3)_2 + 8CO + 3H_2O \rightarrow BaO + 8CO_2 + 2NH_3$	$R_{22} = S^{CO}_{NH_3}\ R_{16}$
$Ba(NO_3)_2 + 8H_2 \rightarrow BaO + 5H_2O + 2NH_3$	$R_{23} = S^{H_2}_{NH_3}\ R_{17}$
$Ba(NO_3)_2 + C_3H_6 \rightarrow BaO + CO_2 + CO + 2NH_3$	$R_{24} = S^{C_3H_6}_{NH_3}\ R_{18}$

$G_1 = (1 + K_{a,1} y_{CO} + K_{a,2} y_{C_3H_6})^2 \cdot (1 + K_{a,3} y^2_{CO} y^2_{C_3H_6}) \cdot (1 + K_{a,4} y^{0.7}_{NO_x})\ T$
$G_2 = 1 + K_{a,5} y_{O_2}$; $G_3 = 1 + K_{a,6} y_{O_2}$; $G_4 = (1 + 0.1\ K_{a,6} y_{O_2})\ (1 + K_{a,7} y_{NO_x})$; $G_5 = 1 + K_{a,8} y_{CO}$

porosity of washcoat, φ^s volume fraction of active washcoat in entire solid phase, ν stoichiometric coefficient, ρ density, ψ surface coverage, Ψ^{cap} maximum storage capacity (mol.m^{-3}, rel. to washcoat volume). In the equations (2), (3) and (5) the reaction rates R_j are employed in dependence on the considered reaction kinetics (cf. Tables 1 and 2). Finite difference method of the Crank-Nicolson type with quasi-linearisation of reaction terms and system decomposition are utilized for numerical solution of the system.

3 NO_x storage and reduction kinetics

The reactions considered in the two studied kinetic models for the NO_x storage and reduction catalyst – the simpler NH_3-selectivity model, and the more complex NH_3-dynamics model – are given in Tables 1 and 2, respectively. Both reaction models include oxidation of CO, H_2 and unburned hydrocarbons (HC), water gas shift and steam reforming, NO reduction, NO oxidation to NO_2, oxygen storage in the form of CeO_2, NO_x storage in the form of $Ba(NO_3)_2$, and desorption/reduction of the stored NO_x by H_2, CO and HC.

The NH_3 selectivity model (Table 1) assumes direct reduction of the stored NO_x to nitrogen or ammonia with given selectivity ratio S_{NH_3}. The model developed earlier (Kočí et al., 2007) and validated by driving cycle tests (Güthenke et al., 2007b) was extended by differentiation of the stored NO_x reduction products to N_2 and NH_3. The selectivity S_{NH_3} is defined here as the ratio of the net NH_3 formation rate to the net N_2 formation rate, with independent values for individual reducing agents (H_2, CO and HC). The more complex

Table 2: Reactions on NO_x storage and reduction catalyst – NH_3 dynamics model.

Reaction step	Reaction rate
$CO + \frac{1}{2}\ O_2 \rightarrow CO_2$	$R_1 = k_1\, y_{CO}\, y_{O_2}/G_1$
$H_2 + \frac{1}{2}\ O_2 \rightarrow H_2O$	$R_2 = k_2\, y_{H_2}\, y_{O_2}/G_1$
$C_3H_6 + \frac{9}{2}\ O_2 \rightarrow 3\ CO_2 + 3\ H_2O$	$R_3 = k_3\, y_{C_3H_6}\, y_{O_2}/G_1$
$CO + H_2O \rightleftharpoons CO_2 + H_2$	$R_4 = k_4\, [y_{CO}\, y_{H_2O} - y_{CO_2}\, y_{H_2}/K^{eq}_{y,4}]$
$C_3H_6 + 3\ H_2O \rightarrow 3\ CO + 6\ H_2$	$R_5 = k_5\, [y_{C_3H_6}\, y_{H_2O} - y^3_{CO}\, y^6_{H_2}/(K^{eq}_{y,5}\, y^2_{H_2O})]$
$CO + NO \rightarrow CO_2 + \frac{1}{2}\ N_2$	$R_6 = k_6\, y_{CO}\, \sqrt{y_{NO}}/G_1/G_2$
$H_2 + NO \rightarrow H_2O + \frac{1}{2}\ N_2$	$R_7 = k_7\, y_{H_2}\, \sqrt{y_{NO}}/G_1/G_2$
$C_3H_6 + 9\ NO \rightarrow 3\ CO_2 + 3\ H_2O + \frac{9}{2}\ N_2$	$R_8 = k_8\, y_{C_3H_6}\, \sqrt{y_{NO}}/G_1/G_2$
$NO + \frac{1}{2}\ O_2 \rightleftharpoons NO_2$	$R_9 = k_9\, [y_{NO}\, y^{0.5}_{O_2} - y_{NO_2}/K^{eq}_{y,9}]/G_1$
$Ce_2O_3 + \frac{1}{2}\ O_2 \rightarrow Ce_2O_4$	$R_{10} = k_{10}\, \Psi_{cap,O_2}\, y_{O_2}\, (\psi^{eq}_{O_2} - \psi_{O_2})$
$Ce_2O_4 + CO \rightarrow Ce_2O_3 + CO_2$	$R_{11} = k_{11}\, \Psi_{cap,O_2}\, y_{CO}\, \psi_{O_2}$
$Ce_2O_4 + H_2 \rightarrow Ce_2O_3 + H_2O$	$R_{12} = k_{12}\, \Psi_{cap,O_2}\, y_{H_2}\, \psi_{O_2}$
$Ce_2O_4 + \frac{1}{9}\ C_3H_6 \rightarrow Ce_2O_3 + \frac{1}{3}\ CO_2 + \frac{1}{3}\ H_2O$	$R_{13} = k_{13}\, \Psi_{cap,O_2}\, y_{C_3H_6}\, \psi_{O_2}$
$NO_2 + \frac{1}{2}\ O_2 + BaO \rightarrow Ba(NO_3)$	$R_{14} = k_{14}\, \Psi_{cap,NO_x}\, y_{NO_2}\, (\psi^{eq}_{NO_x} - \psi_{NO_x})^2$
$2\ NO + \frac{3}{2}\ O_2 + BaO \rightarrow Ba(NO_3)$	$R_{15} = k_{15}\, \Psi_{cap,NO_x}\, y_{NO}\, (\psi^{eq}_{NO_x} - \psi_{NO_x})^2$
$Ba(NO_3)_2 + 5\ CO \rightarrow N_2 + 5\ CO_2 + BaO$	$R_{16} = k_{16}\, \Psi_{cap,NO_x}\, y_{CO}\, \psi_{NO_x}/G_3$
$Ba(NO_3)_2 + 8\ CO + 3\ H_2O \rightarrow BaO + 8\ CO_2 + 2\ NH_3$	$R_{17} = k_{17}\, \Psi_{cap,NO_x}\, y_{CO}\, \psi^2_{NO_x}/G_3/G_5$
$Ba(NO_3)_2 + 8\ H_2 \rightarrow BaO + 5\ H_2O + 2\ NH_3$	$R_{18} = k_{18}\, \Psi_{cap,NO_x}\, y_{H_2}\, \psi^2_{NO_x}/G_3/G_5$
$Ba(NO_3)_2 + \frac{5}{9} C_3H_6 \rightarrow BaO + \frac{5}{3}\ CO_2 + \frac{5}{3}\ H_2O + N_2$	$R_{19} = k_{19}\, \Psi_{cap,NO_x}\, y_{C_3H_6}\, \psi^2_{NO_x}/G_3$
$Ba(NO_3)_2 + 3\ CO \rightarrow 2\ NO + 3\ CO_2 + BaO$	$R_{20} = k_{20}\, \Psi_{cap,NO_x}\, y_{CO}\, \psi_{NO_x}/G_4$
$Ba(NO_3)_2 + 3\ H_2 \rightarrow 2\ NO + 3\ H_2O + BaO$	$R_{21} = k_{21}\, \Psi_{cap,NO_x}\, y_{H_2}\, \psi_{NO_x}/G_4$
$Ba(NO_3)_2 + \frac{1}{3}\ C_3H_6 \rightarrow 2\ NO + CO_2 + H_2O + BaO$	$R_{22} = k_{22}\, \Psi_{cap,NO_x}\, y_{C_3H_6}\, \psi_{NO_x}/G_4$
$Ba(NO_3)_2 + \frac{10}{3}\ NH_3 \rightarrow BaO + 3\ H_2O + \frac{8}{3}\ N_2$	$R_{23} = k_{23}\, \Psi_{cap,NO_x}\, y_{NH_3}\, \psi^2_{NO_x}$
$2\ NH_3 + 3\ NO \rightarrow \frac{5}{2} N_2 + 3\ H_2O$	$R_{24} = k_{24}\, y_{NH_3}\, \sqrt{y_{NO}}$
$2\ NH_3 + \frac{3}{2} O_2 \rightarrow N_2 + 3\ H_2O$	$R_{25} = k_{25}\, y_{NH_3}\, y_{O_2}$
$2\ NH_3 + 3\ Ce_2O_4 \rightarrow N_2 + 3\ H_2O + 3\ Ce_2O_3$	$R_{26} = k_{26}\, y_{NH_3}\, \psi_{O_2}$

$G_1 = (1 + K_{a,1}\, y_{CO} + K_{a,2}\, y_{C_3H_6})^2 \cdot (1 + K_{a,3}\, y^2_{CO}\, y^2_{C_3H_6}) \cdot (1 + K_{a,4}\, y^{0.7}_{NO_x})\, T$

$G_2 = 1 + K_{a,5}\, y_{O_2}$; $G_3 = 1 + K_{a,6}\, y_{O_2}$; $G_4 = (1 + 0.1\, K_{a,6}\, y_{O_2})\ (1 + K_{a,7}\, y_{NO_x})$; $G_5 = 1 + K_{a,8}\, y_{CO}$

NH_3-dynamics model (Table 2) considers in addition to NH_3 formation reactions also the NH_3 decomposition reactions that result in the evolution of moving NH_3 peak on the reduction front boundary during the NSRC regeneration (Kočí et al., 2008, 2009).
The main differences of the two kinetic approaches can be summarized as follows. The NH_3-selectivity model (i) assumes that the NO_x are reduced directly selectively to N_2 or NH_3 depending on temperature and reducing agent (CO, H_2, HC), (ii) uses selectivity defined by experimentally obtained table of values, (iii) is not able to describe detailed dynamics of the ammonia formation within the rich phase as observed in experiments, (iii) requires less computation power. The NH_3-dynamics model (i) considers ammonia both as a product of the NO_x reduction and as an active reduction agent, (iii) predicts the ammonia formation dynamics consistently with experimental observations, and (iii) is computationally more demanding.

4 Results

In this section we compare the simulation results of the simpler NH_3-selectivity model, and the more complex NH_3-dynamics model. Simulations of NSRC operation with periodic alternation of lean and rich inlet mixture switching were carried out for inlet temperature in range 100-500^{o}C, and gas hourly space velocity SV=15 000–120 000 h^{-1}.
Figure 1 illustrates the total amount of NH_3 produced within 10 regeneration periods,

predicted by the two studied models. It can be clearly seen that the NH_3-dynamics model is more sensitive to operating conditions (rich phase length, and space velocity SV).

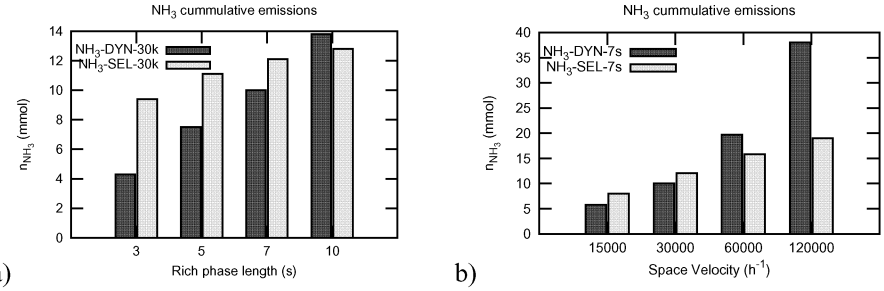

Figure 1: Influence of operating conditions on the NH_3 produced per 10 lean+rich periods. a) Effect of the rich phase length (T^{in} = 300°C, SV = 30000 h^{-1}, 200 s lean phase). b) Effect of the flow rate (T^{in} = 300°C, 200 s lean / 7 s rich phase).

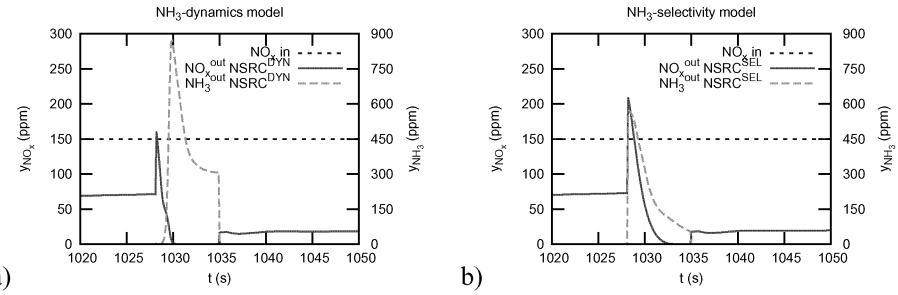

Figure 2: Outlet NO_x and NH_3 concentration during the regeneration phase computed by the a) NH_3-dynamics model and b) NH_3-selectivity model . T^{in} = 300°C, SV = 30000 h^{-1}, 200 s lean / 7 s rich phase.

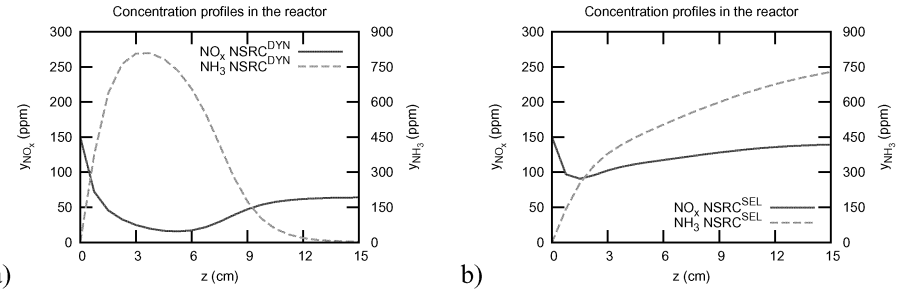

Figure 3: Comparison of NO_x and NH_3 concentration profiles along the reactor 200 ms after the start of the regeneration phase, simulated using the a) NH_3-dynamics model and b) NH_3-selectivity model. T^{in} = 300°C, SV = 30000 h^{-1}, 200 s lean / 7 s rich phase.

Evolution of the NO_x and NH_3 outlet concentrations during the regeneration phase can be seen in Figure 2. For the NH_3-selectivity model, the ammonia peak appears in the same moment as the NO_x peak (Figure 2a), because ammonia is considered as a final by-product of the stored NO_x reduction and not as an reactive intermediate. In the NH_3-dynamics model, the ammonia peak appears after the NO_x peak (Figure 2b), because ammonia is considered both as a product of the stored NO_x reduction, and an active reduction agent.

This sequence of outlet peaks predicted by the NH_3-dynamics model was also observed experimentally in lab reactor (Kočí et al., 2008, 2009).
Figure 3 illustrates gas concentration profiles inside the monolith reactor channel 0.2 seconds after the start of the regeneration. The NH_3-selectivity model predicts ammonia on the outlet almost immediately (Figure 3b). The NH_3-dynamics model considers ammonia also as an active reduction agent, so that the ammonia formed in the front part of the reactor is being used up before it can reach the channel outlet (Figure 3a). The ammonia peak appears at the outlet when the reduction front reaches the rear part of the reactor.

5 Conclusions

The qualitative differences of two approaches to modelling the NO_x reduction dynamics in the NO_x storage catalyst have been shown. For the estimation of integral component conversion (cumulative emissions) around the mean rich phase length the simpler NH_3-selectivity model can be used. The more complex NH_3-dynamics model is consistent with experimentally observed evolution of the outlet NH_3 concentrations (Kočí et al., 2008, 2009), and it is also more sensitive to operating conditions. On the other hand, the increased model complexity results in longer computation times.

Acknowledgements
The work has been supported by the project MSM 6046137306 of the Czech Ministry of Education, and the Grants 104/08/H055 and 104/08/1162 of the Czech Grant Agency.

References

Cumaranatunge L., Mulla S.S., Yezerets A., Currier N.W., Delgass W.N., Ribeiro F.H., 2007, Ammonia is a hydrogen carrier in the regeneration of $Pt/BaO/Al_2O_3$ NO_x traps with H_2. J. Catal. 246, 29.

Epling W.S, Campbell L.E, Yezerets A., Currier N.W., Parks J.E., 2004, Overview of the fundamental reactions and degradation mechanisms of NO_x storage/reduction catalysts. Catal. Rev. 46, 163.

Güthenke A., Chatterjee D., Weibel M., Krutzsch B., Kočí P., Marek M., Nova I., Tronconi E., 2007b, Current status of modelling lean exhaust gas aftertreatment catalysts, in Advances in Chemical Engineering, vol. 33: Automotive Emission Control, Ed. G.B. Marin, pp. 103-211, Elsevier, Amsterdam.

Güthenke A., Chatterjee D., Weibel M., Waldbüsser N., Kočí P., Marek M., Kubíček M., 2007a, Development and application of a model for a NO_x storage and reduction catalyst. Chem. Eng. Sci. 62, 5357.

Kočí P., Schejbal M., Gregor T., Trdlička J., Kubíček M., Marek M., 2007, Transient behaviour of catalytic monolith with NO_x storage capacity. Catal. Today 119, 64.

Kočí P., Plát F., Štěpánek J., Kubíček M., Marek M., 2008, Dynamics and selectivity of NO_x reduction in NO_x storage catalytic monolith. Catal. Today 137, 253.

Kočí P., Plát F., Štěpánek J., Bártová Š., Marek M., Kubíček M., Schmeißer V., Chatterjee D., Weibel M., 2009, Global kinetic model for the regeneration of NO_x storage catalyst with CO, H_2 and C_3H_6 in the presence of CO_2 and H_2O. Catal. Today, submitted.